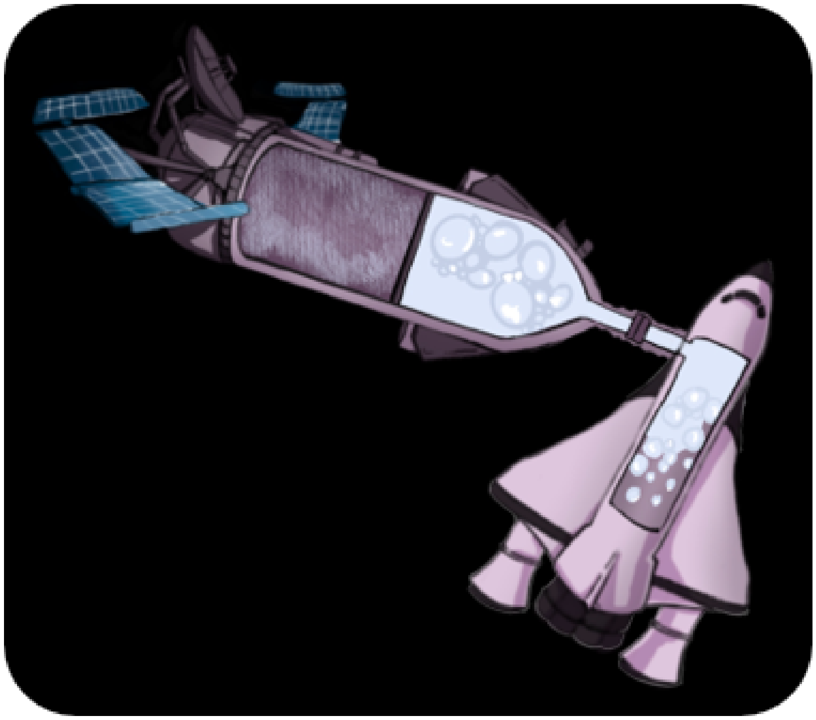

NASA HuLC: Cryogenic Orbital Siphoning System (CROSS)

Department of Mechanical Engineering,
The College of New Jersey

May 28th, 2025

Vaishnavi Adusumilli[1], Mohamed Eladawy[1], Kyle Luis[1], Pierce Rubenstein[1]

Mohammed Alabsi[2], PhD. - Faculty Advisor

Faculty Advisor Signature of Review and Approval

[1] Undergraduate Student, Mechanical Engineering Department, TCNJ, Ewing, NJ, USA
[2] Associate Professor, Mechanical Engineering Department, TCNJ, Ewing, NJ, USA

The College of New Jersey: Cryogenic Orbital Siphoning System (CROSS)

HuLC HUMAN LANDER CHALLENGE

Theme, Objective, and Technical Approach:

Develop and validate a practical method for on-orbit cryogenic propellant transfer utilizing a vapor-driven positive expulsion device.

Major Objective:

Test and validate the transfer process using a piston mechanism and pneumatic pressure control system.

Determine a preliminary expulsion efficiency and redirection to transferal ratio.

Technical Approach:

Create a testing bed featuring the fuel tank, piston, and a destination tank.

Simulate fuel pressurization and transfer using gaseous and liquid nitrogen.

CROSS Graphic:

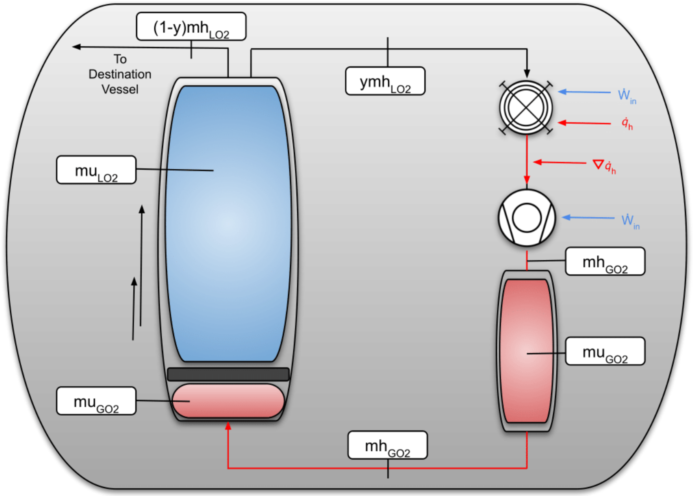

Definitions	
h	Specific enthalpy
u	Specific thermal energy
m	Mass
y	Mass fraction
$\dot{W}$	Power
$\dot{q}$	Heat transfer rate
∇	Gradient

Key	
	High Energy Heating element
	High Energy Compressor
	Piston
	Low Energy thermoelectric Heating

Key Design Details & Innovations:

Key Design Details:

Propellant transfer using piston expulsion device with pressure control

Integrated thermoelectric and resistive elements for vapor generation

Controlling boil-off without the need of helium or other contaminants

Innovation:

PED will be pressurized using fractional amounts of stored fuel into gaseous propellant to actuate a cryogenic vapor actuated pneumatic system (CVAPS) to maintain constant pressure for extended storage periods and for transfer operations.

Summary of Schedule & Costs for Adoption:

Estimated Costs:

$46 million for final device

$83 million including labor and Phase B testing

Path-to-Flight Time:

146 weeks

6/1/2028 Launch Delivery

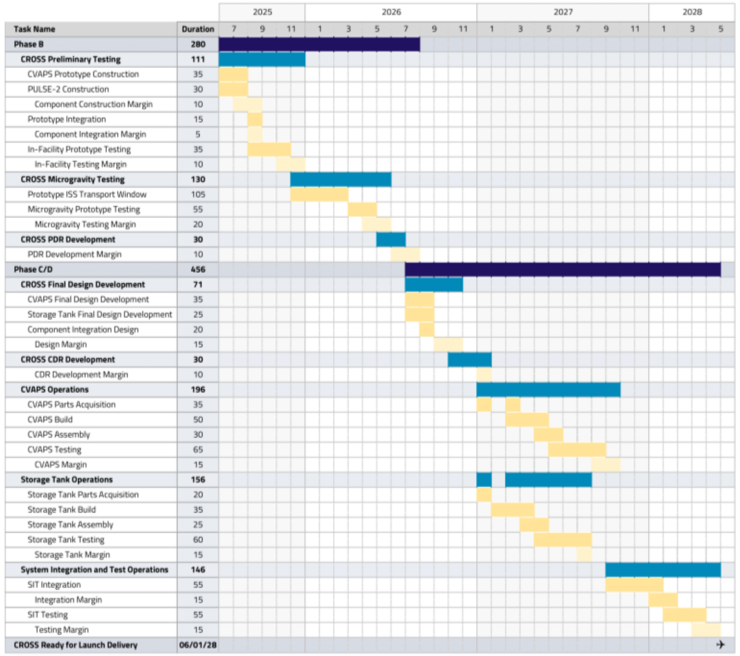

Table of Contents

Executive Summary ... 1
Project Description ... 1
Overview ... 1
Constraints and Guidelines ... 1
Innovation and Capability ... 2
Supporting Analysis ... 4
Piston-Based Positive Expulsion and Microgravity Fluid Dynamics ... 4
Pressure Differential as Passive Driving Mechanism ... 5
Use of Oxygen and Hydrogen as In-System Working Fluids ... 5
The Joule-Thomson Effect and Its Implications ... 7
Thermoelectric Regulation with the Peltier Effect Nodes and Resistive Heaters ... 8
Analog to ISS and CVAP-Like Gas Systems ... 8
Phase Separation and Monophase Delivery ... 8
Verification and Validation ... 8
Testing Apparatus ... 8
Simulation and Fluid Behavior Modeling ... 11
Obstacles ... 12
Technological Assumptions ... 12
Mass and Size Estimates ... 12
Path-to-Flight Timeline ... 13
Advanced Prototype Operations ... 13
Risk Assessment and Mitigation ... 14
Budget Assessment and Operational Cost ... 14
Mission Concept of Operations ... 14
Conclusions ... 15
Appendix ... 16
References ... 22

Executive Summary

The Cryogenic Orbital Siphoning System (CROSS) enables gravity-independent cryogenic propellant transfer using a self-pressurizing, piston-driven architecture. Instead of relying on contaminating pressurants such as helium, CROSS utilizes vaporized oxygen or hydrogen—sourced directly from its own propellant—to drive a cryogenic vapor-actuated pneumatic system (CVAPS).This approach ensures efficient liquid expulsion, minimizes boil-off, and enables stable, slosh-free delivery of liquid propellant to distributed orbital or lunar vessels.

Integrated thermoelectric cooling and resistive heating allow thermal conditioning of the fluid, supporting controlled vapor generation and line preheating. To validate this concept, the Propellant Ullage-Driven Liquid Storage and Expulsion (PULSE) testing apparatus has been developed. using LN_2 , it simulates CVAPS operation and enables for experimental observation of piston movement behavior, pneumatically driven expulsion, and thermal performance under space-analog conditions.

CROSS eliminates the need for helium-based expulsion systems or complex, maintenance-heavy mechanical components, thereby reducing contamination risks and improving overall system reliability. This approach supports safe and consistent propellant transfer with minimal loss—an essential capability for enabling long-duration missions and extending human exploration to the Moon and beyond. Reliable in-space refueling ensures fuel availability for lunar landers, ascent vehicles, and deep-space exploration systems.

Project Description

Overview

This project is focused on advancing a sustainable solution for on-orbit cryogenic propellant transfer in both settled and unsettled microgravity environments. The primary objective is to develop and experimentally validate an efficient and scalable system capable of transferring cryogenic propellants over long durations, supporting NASA's missions to the Moon, Mars, and beyond. This work aligns with the goals outlined in NASA's 2025 Human Lander Challenge (HuLC), which seeks to enhance cryogenic fluid management and transfer systems for extended in-space operations.

The current state-of-the-art in cryogenic fluid transfer primarily addresses short-term storage and transfer, with limited experience in handling large quantities of cryogenic liquids in microgravity or surface tension-dominated environments (Kutter et al., 2006). This project aims to address the gap in understanding the critical transfer phases, such as line chill down, tank chill down, and refueling operations. The proposed concept utilizes vapor pressure—generated through intentional heating—to drive a pneumatically driven piston-based expulsion system. By relying solely on pressure differentials, this novel method minimizes mechanical complexity and efficiently transfers the propellant from storage tanks to its destination.

To validate the proposed concept, a test apparatus is designed and constructed using liquid nitrogen as a model cryogenic propellant. Starting in the first week of June 2025, a series of experiments will gather data that will inform the development of a simulation replicating low Earth orbit conditions, allowing further refinement of the transfer process. This approach will provide key insights into the design of efficient cryogenic transfer systems and contribute to the maturation of technologies necessary for future long-duration missions.

Constraints and Guidelines

Designs must operate effectively in extreme lunar and cislunar environments, withstand launch conditions, and have low mass and power requirements. They must pose no additional risks to crew safety while being capable of surviving both the launch loads and operational challenges of space. To succeed, designs should prioritize simplicity, cost-effectiveness, and novel technical approaches. The proposal must consider realistic implementation plans, particularly accounting for the challenges posed by microgravity, and provide thorough analysis along with clear, unambiguous risk mitigation strategies. Additionally, the design must present realistic timelines and budgets for implementation within 3 to 5 years. CROSS, an acronym for CRyogenic Orbital Siphoning System, aims to utilize what was proposed initially, and provide supporting systems to enable storage and transfer of the liquid propellant.

Innovation and Capability

To address the competing thermal requirements of cryogenic propellant storage and controlled vapor generation in microgravity, CROSS employs a novel thermoelectric preconditioning architecture based on the Peltier effect—adapted to work in conjunction with a piston-driven cylindrical storage vessel. A representation of the Peltier effect is presented in Figure 1.

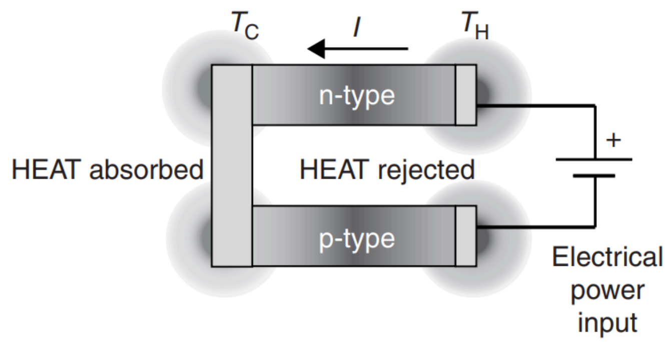

FIGURE 1: Illustration of the Peltier effect (Rowe, 2006)

Because the inner circumference of the tank must remain smooth and unobstructed to allow unhindered piston motion for propellant expulsion and boil-off mitigation, the capillary lines and thermoelectric modules are instead embedded externally along the outer wall of the tank. These lines act as preconditioning channels, guiding a small, metered flow of liquid propellant toward a heating zone. The modules are strategically positioned along these capillary lines, oriented so that their cold sides face the storage tank wall and their hot sides interface with the capillary channels. The cold junctions passively assist in maintaining subcooled liquid temperatures within the tank offsetting any heat leak, thus reducing parasitic boil-off and preserving fluid stability in the absence of convective heat dissipation in space.

Since the thermoelectric modules are arranged as discrete nodal units around the exterior of the tank, the position of the liquid propellant relative to the piston is critical for targeted thermal management. Precise spatial coordination is required to ensure cooling effects are applied exclusively to the liquid region of the tank. Applying cooling to the gaseous volume—located on the opposite side of the piston—could unintentionally reduce the pressure of the working gas or, in extreme cases, cause recondensation into the liquid phase. Such an event would undermine the effectiveness of the pneumatic system and disrupt pressure regulation. To mitigate this, active monitoring of piston position and selective activation of nodal cooling elements are essential for maintaining phase stability and operational reliability.

Simultaneously, the hot sides of the modules incrementally warm the liquid as it progresses through the capillaries. The gradual thermal gradient facilitates preheating without inducing bulk phase change, preparing the propellant for final vaporization downstream. The capillary lines then route the conditioned fluid toward a dedicated heating element where it is rapidly converted into saturated vapor.

The system, following liquid siphoning, is referred to as the Cryogenic Vapor-Actuated Pneumatic System (CVAPS). After vaporization, the gaseous propellant is directed into a single-phase compressor, where it is pressurized to increase its enthalpy and thermodynamic utility. This compression step raises the gas temperature and energy content, enhancing its effectiveness for downstream pneumatic actuation. The high-enthalpy gas is then routed to an intermediate expansion tank, which acts as a thermal and pressure buffer. From this reservoir, the superheated gas can be metered and introduced incrementally into the pneumatic piston system—either to drive liquid expulsion from the primary tank or to regulate internal tank pressure for boil-off suppression. An illustration of CVAPS is provided in Figure 2.

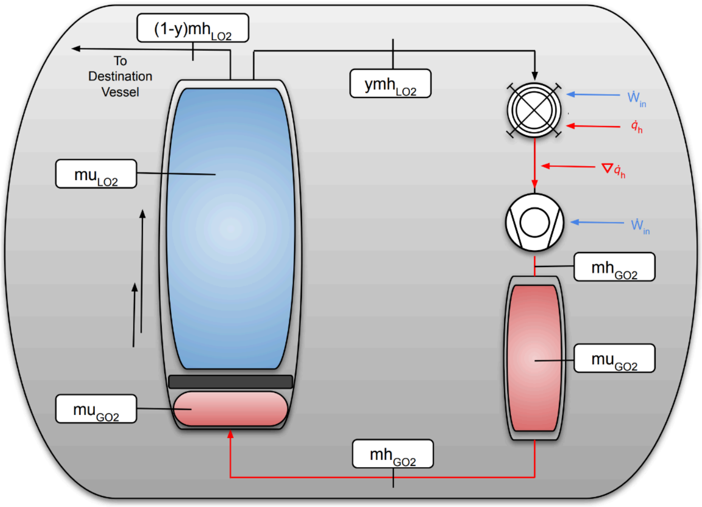

Definitions	
h	Specific enthalpy
u	Specific thermal energy
m	Mass
y	Mass fraction
Ẇ	Power
q̇	Heat transfer rate
∇	Gradient

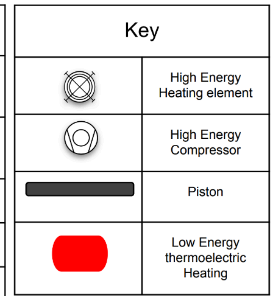

FIGURE 2: CVAPS Basic Layout Illustrating Major Components and Processes

This configuration allows for responsive control over both fluid transfer and thermal stability, supporting a wide range of mission phases including launch, orbital operations, and long-duration cryogenic storage.

The input for pneumatically controlling the amount of gas required—and determining how much vapor must be incrementally sacrificed for actuation—ultimately depends on the pressure differential across the piston and the corresponding systems. To maintain effective fluid expulsion or boil-off suppression, the gaseous side of the piston must sustain a higher pressure than the liquid side, analogous to how ullage gases maintain positive pressure on cryogenic fluids in traditional systems. These pressure differentials are inherently difficult to measure and model precisely, let alone in microgravity conditions, necessitating empirical optimization through rigorous testing and iteration. As a result, the development of a dedicated testing apparatus becomes essential—not only to validate the core functionality of CVAPS, but also to generate critical data that will inform pressure control strategies, gas utilization efficiency, and overall system performance under representative conditions.

To ensure phase purity and stable fluid dynamics throughout the transfer process, the system incorporates a suite of passive and active phase separation mechanisms optimized for microgravity operation. Immediately following the siphoning of liquid propellant into the vapor generation path, a specialized loop geometry is used to promote gravitationally independent phase stratification (Balasubramaniam et al., 2019). This configuration minimizes the ingress of multiphase mixtures into downstream components, preserving the stability of both thermodynamic cycling and pneumatic actuation.

Once the fluid reaches the destination vessel, a centrifugal cyclonic separator—illustrated in Figure 3—is used to extract any residual vapor or entrained liquid slugs from the incoming stream (Balasubramaniam et al., 2019). This component relies on rotational inertia to drive phase separation, with gas and liquid diverted to separate outlets. The result is a clean, monophase delivery to the receiving tank, preventing vapor lock, unbalanced loading, or incomplete tank fill.

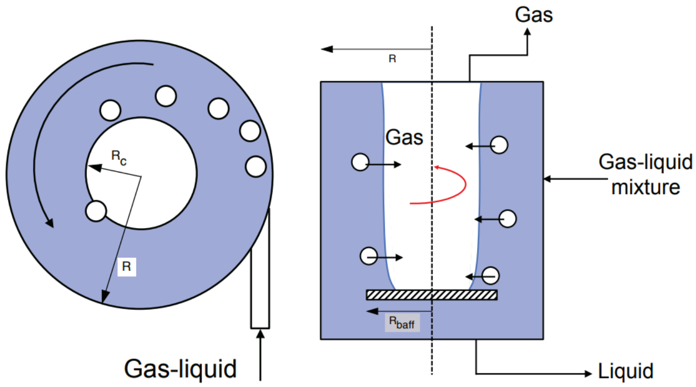

FIGURE 3: Centrifugal Cyclonic Separation of Entrained Two-Phase Flow (Balasubramaniam et al., 2019)

To further ensure flow purity and reduce microbubble-induced instability, hydrophobic membrane segments—illustrated in Figure 4—are integrated along the interior surfaces of the fluidic channels. These membranes allow selective venting of gas bubbles that may have bypassed upstream separation stages (Balasubramaniam et al., 2019).

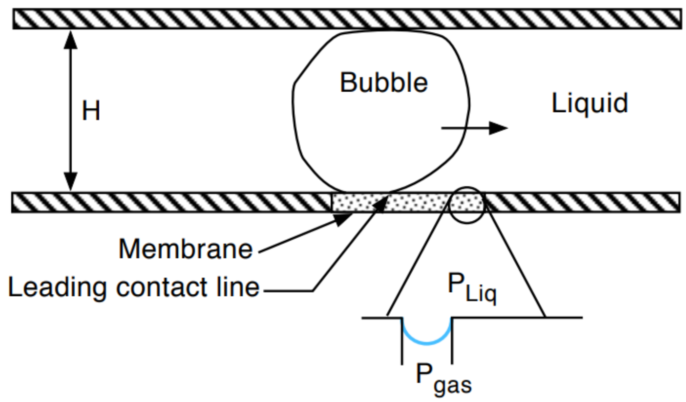

FIGURE 4: Gas bubble passing by a hydrophobic membrane (Balasubramaniam et al., 2019)

Positioned within regions of expected flow recirculation or stagnation, they serve as passive degassing interfaces that eliminate trapped vapor without interrupting bulk liquid movement. This design choice is particularly critical in the absence of gravitational drainage, where even small gas inclusions can significantly disrupt pressure profiles and induce cavitation.

Downstream of the separation zone, a single-phase cryogenic pump is employed to maintain positive flow rate and suppress vapor formation. The use of a pump specifically rated for single-phase operation minimizes the risk of cavitation and enables stable pressure delivery to terminal components, such as modulating valves or terminal collection chambers located in the destination vessel's fuel tank system. By ensuring consistent liquid phase transport throughout the system, this integrated phase control architecture significantly enhances the operational reliability of CVAPS and supports its broader application across varied mission conditions.

Supporting Analysis

The proposed solution architecture draws upon several validated principles in microgravity fluid dynamics, cryogenic propellant management, and thermoelectric regulation. Each subsystem component is supported by empirical precedent or theoretical grounding, detailed as follows.

Piston-Based Positive Expulsion and Microgravity Fluid Dynamics

In microgravity conditions, surface tension dominates over gravitational forces, resulting in non-intuitive fluid configurations such as films, droplets, or bridges adhering to internal surfaces

(Hartwig, 2016). This phenomenon complicates complete expulsion of propellant using traditional drain valves or surface tension-based devices alone. A positive expulsion device (PED), such as a piston, provides a deterministic method for fluid displacement by applying direct mechanical force to the liquid.

The effectiveness of this process can be understood using the Bond number (Bo), a dimensionless parameter defined in Equation 1 as:

$$Bo = \frac{\Delta\rho L_c^2}{\gamma_{LV}} \quad (1)$$

Where **$\Delta\rho$** is the density difference between the liquid and the surrounding phase, **g** is the gravitational (or applied acceleration) force, **L_c** is the characteristic length (such as drop radius or interface curvature), and **γ** is the surface tension (Hartwig, 2016). In microgravity, **g** is near zero, leading to a very low Bond number—meaning surface tension dominates over gravitational forces. However, if the piston applies acceleration, it can increase the effective Bond number locally, making surface tension relatively weaker. This helps the microdroplets coalesce and be driven out with the main bulk fluid. Therefore, the piston not only displaces the bulk liquid but also serves a crucial scavenging function by mobilizing residual droplets adhered to internal surfaces.

NASA has historically employed diaphragms and bladder tanks for positive expulsion in spacecraft (Hartwig, 2016) but rigid-body pistons offer improved structural integrity for large cryogenic volumes and enable precise control over residual fluid scavenging. Piston-induced acceleration can locally increase the Bond number, as previously described, mitigating surface adhesion effects and consolidating dispersed microdroplets (Jenson et al., 2009).

Pressure Differential as Passive Driving Mechanism

The reliance on pressure differentials for fluid transport is a cornerstone of spacecraft propellant systems, including Integrated Vehicle Fluids (IVF) and Pressure Fed Systems (PFS) (Rudman & Austad, 2002). By leveraging naturally occurring or thermally induced phase pressure differences between cryogenic liquids and their corresponding vapors, the system reduces reliance on mechanical actuation.

In CVAPS, a thermally preconditioned phase transition creates high-pressure gaseous propellant, which then serves as a dual function: pneumatic action and tank pressurization. This configuration mimics features of ullage control used in the Centaur Upper Stage and NASA's RL10 engine systems, where GH_2 and GO_2 are used for tank pressurization and engine purging (Rudman & Austad, 2002).

Use of Oxygen and Hydrogen as In-System Working Fluids

The CROSS system eliminates the need for foreign working fluids such as helium by utilizing the cryogenic propellants themselves—LO_2 and LH_2—as both thermodynamic and pneumatic working media. This unified approach improves fluid compatibility, eliminates the risk of system contamination, and supports a closed-loop fluid architecture optimized for propellant transfer operations.

Both LO_2 and LH_2 exhibit favorable properties for this dual role. These include high latent heats of vaporization, large volumetric expansion ratios, and low viscosities in both liquid and gas phases. Their behavior under throttling and controlled compression/expansion cycles further enables their use in pressure management, thermal energy transfer, and mechanical actuation tasks. A summary of relevant thermophysical properties is presented in Table 1.

TABLE 1: Thermophysical Properties of LO_2 and LH_2 (NIST, n.d.)

Property	LO_2	LH_2	Impact
Boiling Point at 1 atm	90.19 K	20.28 K	Much higher boiling point for LO_2
Latent Heat of Vaporization	213 kJ/kg	446 kj/kg	Energy required to vaporize 1 kg of liquid
Density (liquid at boiling point)	1140 kg/m^3	70.85 kg/m^3	Much lower density for LH_2, contributing to expansion
Density (gas at 1 atm, Boiling T)	4.43 kg/m^3	0.0899 kg/m^3	Significant volumetric expansion
Volumetric Expansion Ratio (liq→gas)	860:1	845:1	At STP
Dynamic Viscosity (liquid)	0.2 mPa-s	0.013 mPa-s	LH_2 is extremely low viscosity
Dynamic Viscosity (gas at 300 K)	20.1 µPa-s	8.9 µPa-s	Low viscosity supports ease of flow
Joule-Thomson Coefficient at STP (μ_{JT})	+0.3 K/bar	-0.06 K/bar	Lo_2 cools on expansion, LH_2 slightly warms
Specific Heat Capacity (gas at 300 K)	0.918 kJ/kg-K	14.3 kJ/kg-K	High C_p of GH_2 supports strong thermal buffering

The following describes the 8-stage closed-loop process employed by the CVAPS system to utilize LO_2 and LH_2 as internal working fluids:

- **Stage 0**: Cryogenic Storage **(P_1,V_1)**
  - Liquid propellant is stored in a cryogenic tank maintained at constant pressure **(P_1)** and volume **(V_1)**, with thermal insulation and a movable piston or diaphragm separating the ullage gas from the liquid. The piston ensures constant pressure and suppresses boiling due to heat ingress.
- **Stage 1**: Isobaric Siphoning
  - A small mass of liquid at **(P_1,V_1)** is withdrawn into the siphon line. The piston prevents pressure drop and maintains isobaric withdrawal.
- **Stage 2**: Isenthalpic Expansion and Joule-Thomson (J-T) Throttling
  - The liquid flows through a pressure-reducing orifice or valve where pressure drops from **P_1** to **P_2**. Since the fluid is still in liquid phase, it's an isenthalpic liquid throttling where $\Delta h = 0$ (throttling). This step does not cause phase change or significant temperature variation but plays a crucial role in preventing upstream heat leak. Because no external heat is introduced and enthalpy remains constant, this effectively isolates the cryogenic tank thermally, preserving its low-temperature state.
- **Stage 3**: External Heating and Compression Preparation **(P_3,V_3)**
  - Downstream of the throttling point, heat is deliberately introduced to vaporize the liquid, represented in Equation 2:

$$q = \int_{T_{sat}}^{T_3} C_p dT \quad (2)$$

    Here, the heat input must exceed the latent heat of vaporization to convert the liquid to gas and raise it to the desired temperature. The resulting gas is now at slightly elevated pressure and enthalpy, ready for mechanical compression.

- **Stage 4:** Gas Compression **(P_4,V_4)**
  - The vapor is compressed from **(P_3,V_3)** to **(P_4,V_4)**, increasing its enthalpy and making it suitable for downstream use in pressurization and pneumatic actuation. Assuming near-isentropic compression, energy, **W**, for an ideal gas, both pressures are defined by in Equation 3 as:

$$PV^{\gamma} = \text{constant} \rightarrow \frac{T_4}{T_3} = \left(\frac{P_4}{P_3}\right)^{\frac{\gamma-1}{\gamma}} \qquad (3)$$

    Where **P_3, V_3, T_3** is at the compressor inlet and **P_4, V_4, T_4** is at the compressor outlet. **γ** is the ratio of specific heats (about 1.41-1.43 for O_2 and H_2). This relation assumes adiabatic, reversible compression (no heat loss, no friction) and describes the thermophysical relationship between the two stages.
- **Stage 5:** Transfer to Expansion Tank **($P_5 = P_4 \rightarrow P_6 < P_5$)**
  - Gas exits the compressor and fills a downstream expansion tank. Because the expansion tank is at a lower pressure **($P_6 < P_5$)**, the flow is driven by the pressure gradient. The tank volume **V_6** is significantly larger, accommodating pressure regulation and energy storage.
- **Stage 6:** Stored Expansion Readiness **(P_6, V_6)**
  - The expansion tank retains pressurized gas at **(P_6,V_6)** under regulated temperature and insulation. The tank volume is higher than the compressor output line, allowing for adequate storage and buffer capacity.
- **Stage 7:** Piston Actuation **($P_7 < P_6$)**
  - When needed, the stored gas is introduced to the opposite side of the piston in the storage tank. If **(P_7<P_6)**, the gas expands and does work where it either supports the displacement of liquid cryogen for transfer or active pressurization of the ullage space to suppress boil-off during orbit or launch conditions.

The system adheres to the First Law of Thermodynamics via conservation of energy and the Second Law of Thermodynamics where entropy increases with irreversible expansion, throttling, and controlled heat transfer. Furthermore, the propellants are both viable in this role where their expansion ratio and high enthalpic properties make them great candidates for CVAPS. This architecture supports a fully integrated propellant-handling and pressure management system using only the native fluids.

The Joule-Thomson Effect and Its Implications

The Joule-Thomson (J-T) effect describes the temperature change of a real gas when it undergoes an isenthalpic (constant-enthalpy) expansion, typically through a flow restriction or throttling device . The magnitude and direction of the temperature change are governed by the Joule-Thomson coefficient and is defined in Equation 4 as:

$$\mu_{JT} = \left(\frac{\partial T}{\partial P}\right)\Big|_{H} \qquad (4)$$

This coefficient, expressed in K/bar, defines how temperature varies with pressure during an isenthalpic process . If $\mu_{JT} > 0$, the gas cools during expansion (as is the case for oxygen under cryogenic conditions); if $\mu_{JT} < 0$, the gas warms (as hydrogen does at temperatures above 220 K).

From first principles, μ_{JT} can also be expressed in terms of specific heat and real-gas properties, evidenced in Equation 5 (Gans, 1992):

$$\mu_{JT} = \frac{1}{C_p}\left[T\left(\frac{\partial V}{\partial T}\right)\Big|_{P} - V\right] \qquad (5)$$

Where V is the control volume, and Equation 4 is rearranged with assumptions being that H is held constant (and therefore dH is 0 due to the process being isenthalpic). This relationship connects microscopic gas behavior to macroscopic thermal outcomes. During Stage 2 of CVAPS, isenthalpic expansion occurs as liquid cryogen passes through a pressure drop from the storage tank, preserving Δh = 0. This J-T throttling effectively isolates the cold-side tank thermally, preventing heat leak and reinforcing adiabatic assumptions at the storage interface. For LO_2, this expansion results in cooling, aiding in cryo-stability. FOr LH_2, which exhibits a slightly negative μ_{JT}, at cryogenic temperatures, the expansion causes mild warming, which is manageable due to downstream heat control.

The J-T effect also applies during transitions at the expansion tank. When gas flows from the compressor outlet (Stage 5) into the expansion tank, it undergoes pressure relief and slight isenthalpic expansion, depending on flow restriction and thermal insulation. When gas is later released (Stage 7) from the expansion tank into the piston line, it again experiences throttling, governed by the same enthalpic principles and J-T behavior.

In both cases, these transitions ideally remain isenthalpic and are thermodynamically relevant because they involve real gas effects without external heat or work and supports the system's adherence to being supported and governed through pressure differential input using only native fluids as working media.

Thermoelectric Regulation with the Peltier Effect Nodes and Resistive Heaters

Thermoelectric cooling using the Peltier effect has been explored for low-power spacecraft thermal management applications and is increasingly viable due to advances in thermoelectric materials (Rowe, 2006). In the CVAPS configuration, its modularity and solid-state nature offer unique advantages in a microgravity cryogenic setting where convective cooling is ineffective.

In this architecture, thermoelectric modules serve a dual function: cooling localized tank wall regions to suppress boil-off and simultaneously heating gas-phase propellant in adjacent transfer lines by exploiting the Peltier hot side. This bidirectional control allows thermal conditioning of both liquid and gaseous phases within a compact footprint, optimizing thermal gradients based on piston location and flow state.

To ensure complete vapor saturation before the gas enters the compressor, a dedicated resistive heating element is included in-line after the thermoelectric segment. NASA commonly uses polyimide resistive heaters (Custom Heaters & Research, n.d.) for this function in long-duration orbital environments due to their lightweight, flexible, and radiation-resistant construction. These heaters can deliver precise heat flux and are compatible with cryogenic systems where uniform heating of GH_2 or GO_2 is required. This integrated thermal management approach ensures that gaseous working fluids are fully conditioned—minimizing risk of compressor cavitation and enhancing pneumatic consistency across the entire operation.

Analog to ISS and CVAP-Like Gas Systems

CVAPS design principles are comparable to the ISS Ammonia Thermal Control System (ATCS) and Gas Pressurization Systems used in Environmental Control and Life Support System (ECLSS) modules, which rely on phase-conditioned gases for loop pressurization, purge, and circulation (ERASMUS Centre, n.d.). The modular and redundancy-driven nature of these systems validates the distributed thermoelectric and pneumatic control logic used in CVAPS.

Phase Separation and Monophase Delivery

NASA's cryogenic fluid management (CFM) roadmap outlines the importance of active and passive phase separators to ensure monophase delivery (George C. Marshall Space Flight Center [MSFC], n.d.). The use of cyclonic separators and hydrophobic membranes aligns with these strategies and mimic elements used in zero boil-off (ZBO) and propellant transfer experiments aboard the ISS and STS (NASA Science Editorial Team, 2024).

Hydrophobic membrane venting, in particular, has been validated under parabolic flight and drop tower tests (Balasubramaniam et al., 2019), demonstrating efficacy in removing microbubbles and minimizing cavitation during microgravity transfers.

Verification and Validation

Testing Apparatus

To validate the performance of CVAPS, a dedicated testbed—designated the Propellant Ullage-Driven Liquid Storage and Expulsion (PULSE) apparatus—has been developed. PULSE simulates the CVAPS operation and allows detailed examination of pressure differential requirements and cryogenic fluid transfer efficiency under conditions representative of in-space application. At the core of the apparatus is a pneumatically actuated expulsion piston, designed to transfer cryogenic liquid (LN_2) from a simulated storage chamber to a downstream destination tank, illustrated using Solidworks 2025 in Figure 5. Several physical prototypes are presented in Figure A7 of the Appendix. A 3D model is presented in Figure 6.

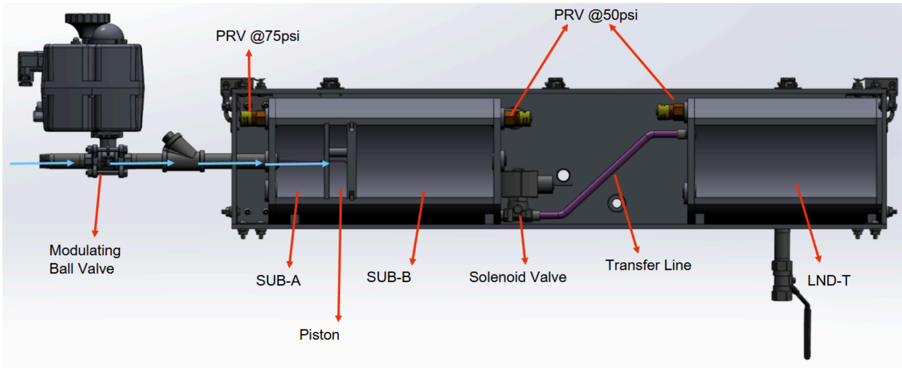

FIGURE 5: PULSE Apparatus Solidworks Diagram

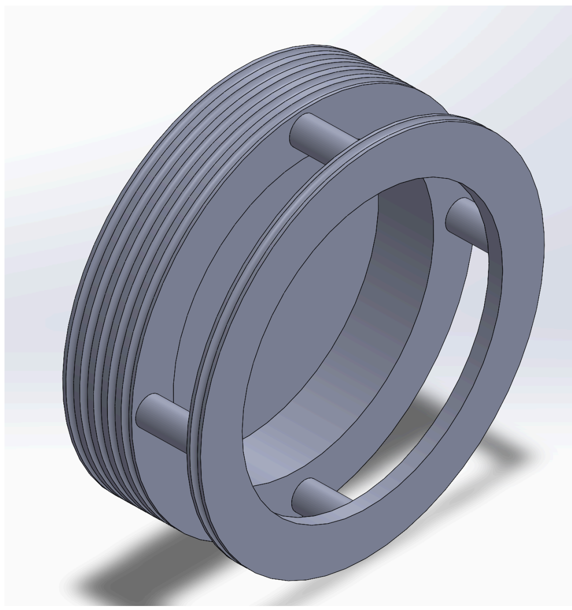

FIGURE 6: A 3D model of the piston used to expel LN_2

The piston, made of 6061 aluminum, resides within a smooth hydraulic steel cylinder and separates two regions of nitrogen: a gaseous chamber (SUB-A), which is supplied with externally sourced gaseous nitrogen GN_2 to simulate ullage pressurization, and a cryogenic liquid chamber (SUB-B), which contains LN_2 to be expelled. While CVAPS provides the expulsion method, a physical barrier is still recommended to prevent a gas-liquid mixture. The chamber orientation is horizontally inclined to minimize gravitational artifacts during fluid displacement, mimicking the low-gravity environment intended for CVAPS operation. Further views and the current pictures of this apparatus are found in Figures A1 to A6. To regulate gas flow into SUB-A, a modulating ball valve utilizes pressure differential feedback to respond accordingly. GN_2 is metered into the gas chamber based on live readings from a network of pressure sensors strategically placed along the piston face (SUB-A), the opposing wall (SUB-B), and the destination tank (LND-T), with the full control system illustrated in Figure 7.

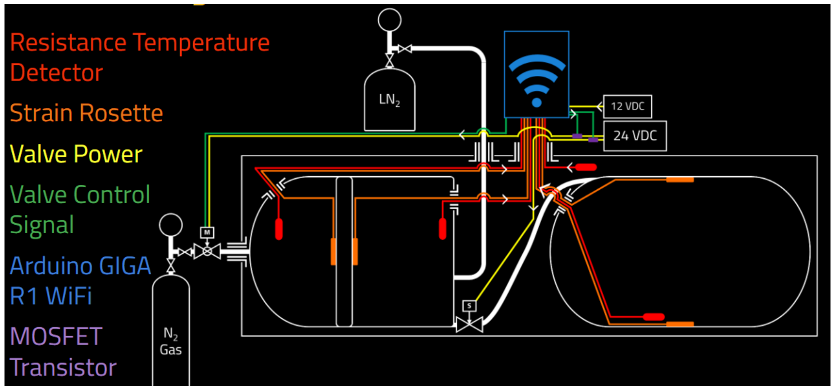

FIGURE 7: PULSE Control System Wire Routing Diagram

These sensors allow precise control of the pneumatic actuation process and enable quantification of the gas volume required to initiate and sustain cryogenic fluid transfer—an essential performance metric for optimizing vapor utilization within CVAPS.

In order to obtain accurate measurements, strain rosettes and cryogenic-rated temperature sensors are integrated along the piston assembly and along the transfer line connections to monitor structural response and thermal behavior throughout the operation. These instruments provide insight into in-line chilldown performance and potential heat leakage into the cryogenic fluid portions—factors critical to maintaining phase integrity and minimizing boil-off.

One of the central goals of the PULSE campaign is to establish the expulsion efficiency ratio, noted as $\eta_{expulsion}$, between the amount of gaseous propellant required for actuation and the volume of liquid successfully expelled—a metric that determines the performance of propellant management devices (Hartwig, 2016). In doing so, the PULSE testing not only demonstrates the feasibility of gas-driven cryogenic expulsion but also provides a critical feedback loop for optimizing CVAPS performance across a range of mission conditions.

Within the pressurized vessel, the gaseous chamber, SUB-A, is supplied with an external source of GN_2 to mimic the proposed CVAPS system. The fluid within the LN_2 chamber, SUB-B, is expelled through an inclined transfer line to minimize gravity effects. The design of PULSE has a focus on collecting data to find the ratio between extracted propellant from CVAPS to its expelled counterpart in order to verify its concept. In the use of the pneumatic system, strain rosettes and temperature sensors are applied along the piston face within SUB-A, the opposing wall in SUB-B, as well as the destination tank, LND-T.

The locations of pressure sensors are chosen to be along the piston face along the gas chamber, SUB-A, and opposing wall of the liquid chamber, SUB-B, with a final one in the destination tank, LND-T, for processing pressure readings, allowing the modulating valve's differential pressure control scheme to manage the supply entering the apparatus's gas chamber. A modulating ball valve regulates gas flow based on pressure differentials measured by the previously mentioned rosettes, releasing only the amount of gas necessary to actuate the piston for fluid expulsion. Determining the gas volume required to move the piston serves as proof of concept and helps quantify the amounts needed to ensure effective expulsion from the CVAPS. Similarly, temperature sensors are strategically placed along both sections of the pneumatic system and the destination tank, not only to monitor for potential heat leak inefficiencies, but also to gather critical data for analyzing the thermophysical properties of the fluid before and after transfer.

The entire PULSE apparatus is insulated within a vacuum chamber, constructed using G-10 "Garolite" composite panels, with three layers of Mylar "space blankets" to minimize thermal radiation effects. An acrylic panel serves as a viewing window for testing and observation. To ensure airtight sealing and structural integrity under vacuum conditions, silicone and specialized cryogenic epoxy are applied along all edges and mating surfaces while the panels are secured using nuts, bolts, and sealing washers that fit into the machined panels. The chamber's structure is secured using corner mounts, eliminating unnecessary conductive heat transfer. An on-site vacuum pump provides vacuum conditions, achieving 15 microns (0.0000074 psia) in an ideal sealed environment. To establish a highly cryogenic environment, the system is pre-chilled prior to operation, and testing occurs in a low-light laboratory setting to further limit external thermal influence.

Finally, the control system known as SCRIPT (System for Cryogenic Investigative Procedures at TCNJ) oversees the operations, utilizing strain gauge pressure transducers and resistance temperature detectors to regulate the PULSE apparatus and collect real-time data. The core of this system is a feedback control loop, using the pressure difference between SAT-T and LND-T to determine the position of the GN_2's modulating control valve. Additional pressure and temperature sensors are installed to collect data for calculation of the expansion ratio and thermodynamic analyses. The SCRIPT is wifi-enabled and hosts all functionality on a local web server, allowing data to be monitored while maintaining a safe testing environment. For optimal wifi connection and easy access to electrical connections, the SCRIPT is located outside the chamber, with wiring feedthroughs allowing signals to pass from inside each tank to the rest of the system. The wiring diagram is presented in Figure A9 of the Appendix.

Simulation and Fluid Behavior Modeling

To support experimental data collection, computational fluid dynamics (CFD) was employed to analyze fluid behavior under test-mimicking conditions. ANSYS Fluent was selected due to its availability, user-friendly interface, and suitability for initial simulations, with plans to address computational limitations in future iterations. Custom geometries replicating the actual transfer apparatus were created to enable both flow visualization and iterative simulation. However, due to limitations in available cryogenic flow rate sensors, verification of results still relies primarily on strain rosettes for pressure and temperature data acquisition. Simulations were conducted across a range of transfer velocities, consistent with the ball valve modulation control scheme, to generate a data set representing total pressure losses along the transfer line. As shown in Figure 7, the pressure loss vs. transfer velocity curve confirms that all values remain below the pressure relief valve's maximum differential pressure of 25 psi (172.3 kPa), ensuring system safety margins are maintained.

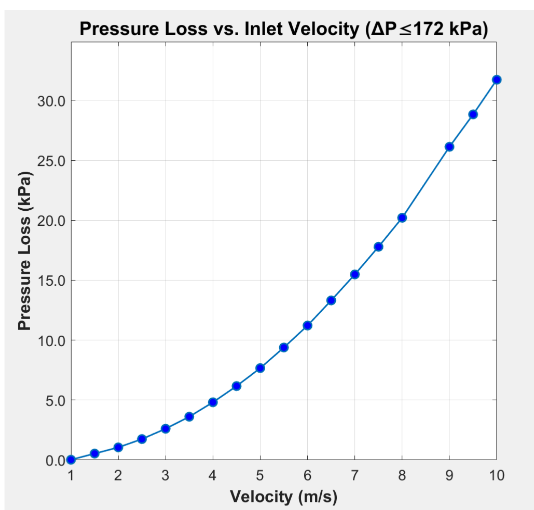

FIGURE 7: Pressure and Velocity Relationship in Transfer Line

The simulated model replicates the internal geometry of the transfer line, as shown in Figure A10 of the Appendix, with boundary conditions matching expected flow conditions during PULSE operation. A representative simulation was conducted at an inlet velocity of 5 m/s, with a total elapsed time of 0.053 seconds, to examine fluid behavior at the elbows of the transfer line, where flow separation and directional changes are most pronounced. A secondary simulation was performed on the destination tank

(LND-T) to capture effects resulting from the expulsion process. A range of inlet velocities—from 1 m/s to 15 m/s—was evaluated to assess the influence of varying expulsion rates on internal tank behavior, with corresponding results presented in Figures A11 and A12 of the Appendix. To capture the highly dynamic nature of cryogenic fluid, an explicit time formulation was utilized, resulting in a high-fidelity simulation of internal flow dynamics within the destination vessel. Although ANSYS Fluent offers a user-friendly interface for CFD analysis, its limited flexibility poses constraints on advanced simulation capabilities. In contrast, OpenFOAM provides extensive customization potential but demands a deeper understanding of solver architecture, boundary condition scripting, and numerical method tuning. Despite these challenges, both tools proved valuable for capturing the intricate fluid dynamics of the PULSE system, reinforcing their utility in guiding experimental design and informing overall system optimization.

Looking ahead, OpenFOAM is being integrated with ANSYS Transient Thermal to account for thermal discrepancies and heat transfer effects in the transfer line, particularly under cryogenic conditions. These simulations aim to align with temperature data collected from onboard sensors for improved validation accuracy.

Obstacles

CROSS must be able to withstand the extreme conditions of space while also integrating seamlessly with existing propellant transfer methods. It needs to maintain precise temperature gradients for cryogenic propellants, despite the absence of convective cooling, and prevent parasitic boil-off while ensuring controlled vaporization for pneumatic actuation. In microgravity, it must overcome challenges like droplet adhesion and incomplete tank evacuation. Phase separation techniques—cyclonic or hydrophobic—must be validated under realistic conditions.

Particular attention must be given to the piston and sealing mechanisms, which need to function reliably at cryogenic temperatures while resisting thermal cycling, radiation, and launch-induced vibrations. Testing under simulated space conditions, such as thermal vacuum chambers and microgravity environments, is essential to identify and address any material or design weaknesses early in development.

Technological Assumptions

CROSS operates on key assumptions to ensure reliable propellant transfer in microgravity. Before launch, the system is pressurized with CVAPS to stabilize cryogenic fluids and prevent sloshing during ascent. Advanced thermal protection, including multi-layer insulation and reflective coatings, maintains proper temperatures throughout all mission phases, while solar arrays with robust energy storage provide continuous power, even during eclipses.

The system relies on automated IDSS-compatible docking systems with machine vision and force sensors for precise connections without crew intervention. The design incorporates redundant fail-safes for emergency separation and assumes stable inertial properties to prevent unwanted spacecraft motion during transfers. Microgravity operations depend on controlled ullage gas management to enable piston functionality while avoiding vapor ingestion.

These technologies will undergo rigorous ground testing followed by orbital validation on the International Space Station. The system's pressurization, thermal management, and docking capabilities must all perform flawlessly to ensure successful propellant transfers for Artemis missions and deep-space exploration. Continuous monitoring and multiple redundancy layers address potential risks throughout all mission phases.

Mass and Size Estimates

The PULSE prototype is currently configured for tabletop simulation, with its vacuum chamber dimensioned at 8” × 8” × 36” and weighing approximately 40 lbs. This bench-scale implementation focuses on validating core operational principles while maintaining compact form factor requirements. In a full-scale deployment, the system would incorporate two critical expansions: the piston assembly within the storage vessel and the CVAPS (Controlled Vapor Actuation and Pressure System) components. The piston would span the complete diameter of the storage vessel, with its thickness optimized solely to accommodate edge seals rather than structural load-bearing. Additionally, the piston would be supported in its orientation via standoffs and a piston skirt, similar to the prototype, providing true parallel form within the vessel. The CVAPS system's three external components would be arranged in parallel configuration along the tank's longitudinal axis, minimizing radial footprint through strategic packaging that leverages dead space around the primary vessel.

The size of the storage tanks is based on the Human Lander Challenge's guidelines, with dimensions approximately 6 meters in diameter and up to 10 meters in height. Since the piston spans the tank's diameter, its mass must be considered in the total system weight. To reduce its contribution, it is recommended that the piston be manufactured from a composite material. NASA-standard composite materials have an estimated density of 1600 kg/m³ (Goodfellow, 2003). Using a 33:1 scale factor, the piston is estimated to weigh approximately 21,300 kg (~47,000 lbs). The inner tank is assumed to be constructed from an aluminum alloy commonly used in cryogenic propellant storage (Merino et al., 2017). With the same scaling factor, its mass is estimated at around 2,600 kg (~5,730 lbs). The skeletal outer structure, also assumed to be made from composite material, contributes an estimated 374 kg (~824 lbs). Compressors are relatively lightweight compared to other components. Based on typical cryogenic liquid and gas compressor specifications, their mass ranges from 2 to 10 kg, depending on the manufacturer (Nast et al., 2014). An additional 250 kg is allocated for thermal lines and electronics, which include sensors, thermoelectric modules, and power systems.

For insulation, multilayer insulation (MLI) is used—based on thermal protection found on the Space Shuttle's external tank (NASA, 2005). By applying the ratio of thermal protection mass to the surface area of the Shuttle's tank, the MLI mass is estimated to be approximately 800 kg (~1,760 lbs). Finally, with the inclusion of an expansion tank and applying a 1.25 multiplier to account for any unaccounted components—such as fittings, seams, overlaps, or attachment methods—the total estimated dry mass of the system is just under 32,000 kg. Since there is a requirement for two systems—LO_2 and LH_2— the total mass of both systems is roughly 64,000 kgs (~141,000 lbs).

Path-to-Flight Timeline

An estimated path-to-flight timeline, presented as Figure A13 in the Appendix, has been developed following NASA's Schedule Management Guidelines and Single-Project Program Life Cycle. This timeline predicts a launch delivery readiness date of about 150 weeks, presuming that design selection at the HuLC Forum signifies successful meeting of Pre-Phase A and Phase A requirements. Since both piston-based PEDs and autogenous pressurization modeling have undergone ample development, only an updated prototype is expected to be needed in Phase B.

Advanced Prototype Operations

As the current PULSE apparatus has been designed as a proof-of-concept for the autogenous pressurization of a positive expulsion device, NASA's first step in adopting the CROSS for Artemis missions is the development of an advanced prototype. This device will need to cover operational capabilities for which the current model has not been designed, with key focuses on validating the CVAPS and determining an optimal piston design. A scale model of the storage tank and piston, similar to the PULSE, will be developed alongside a simplified CVAPS to support tests that allow for dimensional analyses to take place.

Initial development of the advanced prototype will take place in its separate components, with a system integration stage occurring before test operations take place. These tests will be split between ground and microgravity testing phases to provide validation for a wide range of environments. For ground tests, the main goals will consist of finalizing piston material and shape, ensuring piston sealing abilities, confirming CVAPS model operability, and performing boil-off and slosh analyses. While these tests may be done at Marshall Space Flight Center's Sunspot Thermal Vacuum Testing Facility, a wider range of tests can be performed utilizing Goddard Space Flight Center's SEC and Space Environment Simulator.

The main goal of the microgravity testing phase is to confirm the viability of the CROSS' use of thermoelectric cooling and heating, vapor compression and storage, pneumatic actuation, cyclonic separators, and hydrophobic membranes. Additionally, these tests will be used to demonstrate CROSS' ability to perform its siphoning and transfer operations in zero gravity. These tests will be performed on board the International Space Station utilizing the advanced prototype, with an estimation that the mechanism can be transported on a resupply mission this winter or the following spring. Allowances for an appropriate launch window have been included in the timeline, and an extended testing time frame has been allotted to perform tests safely.

Risk Assessment and Mitigation

An additional goal of both testing phases is the identification of risks associated with the CROSS design. As the system relies on a piston expulsion device, the two largest potential risks are incomplete sealing and piston misalignment. To ensure the piston seals along its full circumference at all points of its traversal, two design components will be used. First, the tank will be supported by structural webbing, which will be manufactured as part of the tank walls. These stiffeners will prevent natural flexure of the tank walls, the major source of piston unsealing. Secondly, an engine block inspired outer casing will be used to further support the tank walls. The tank—with its thermoelectric nodes and phase change lines installed—will be slotted into this outer casing, which will include additional structural webbing. To allow for service access to the nodes and lines after a successful mission, the casing will be equipped with service panels.

As these supports will allow the tank to maintain a uniform shape, they will also prevent one source of piston misalignment. However, to best ensure the horizontally aligned traversal of the piston, an additional piston "skirt" will be utilized. This structure, separated from the main piston using a set of standoffs as in the PULSE device, will be installed on the gas side of the tank and allow for highly improved stability without major increases in piston mass or friction.

Budget Assessment and Operational Cost

The PULSE system cost approximately $8,000 to develop and test this novel concept. This budget reflects significant impacts from manufacturing constraints and development costs inherent to smaller university-based research environments. Working with cryogenic fluids also drove up the cost of electronic components, as specialized materials and interfaces are needed to ensure safe and reliable operation in extreme temperature conditions. The procurement of cryogenically compatible sensors, insulated wiring, and vacuum-rated materials contributed notably to the overall expenses.

Utilizing an adjusted version of the NASA Instrument Cost Model (Mrozinski, 2020), in conjunction with the mass and power estimates previously described, integrating the CROSS with NASA's existing systems is projected to cost about $46 million. Factoring in labor and Phase B testing of the CVAPS system, the overall cost of developing the CROSS over the course of the proposed timeline is about $83 million.

While the initial costs are significant, CROSS is designed for reusability, reducing long-term expenses across multiple missions. This will eventually result in a per-mission cost less than that of helium-based pressurization systems, which currently cost approximately $2 million per mission as of October 2024 . This cost estimate specifically applies to Artemis program missions and does not account for potential integration with other NASA programs or commercial spaceflight initiatives. Future modifications may be required for broader applications.

Mission Concept of Operations

CROSS enables autonomous cryogenic propellant transfer in microgravity. Before launch, the system is pressurized to prevent sloshing during ascent. Once in orbit, real-time monitoring verifies system stability. When a destination vehicle requests fuel, automated docking establishes a secure connection. The system then diverts a small propellant portion, vaporizing it to drive a piston that pushes the remaining liquid through transfer lines while scavenging tank residues. Advanced separators ensure pure liquid delivery. Post-transfer, pressures equalize before clean disconnection. The system can vent or recycle residual gas. A simple table depicting a standard CROSS mission timeline is seen in Table 2.

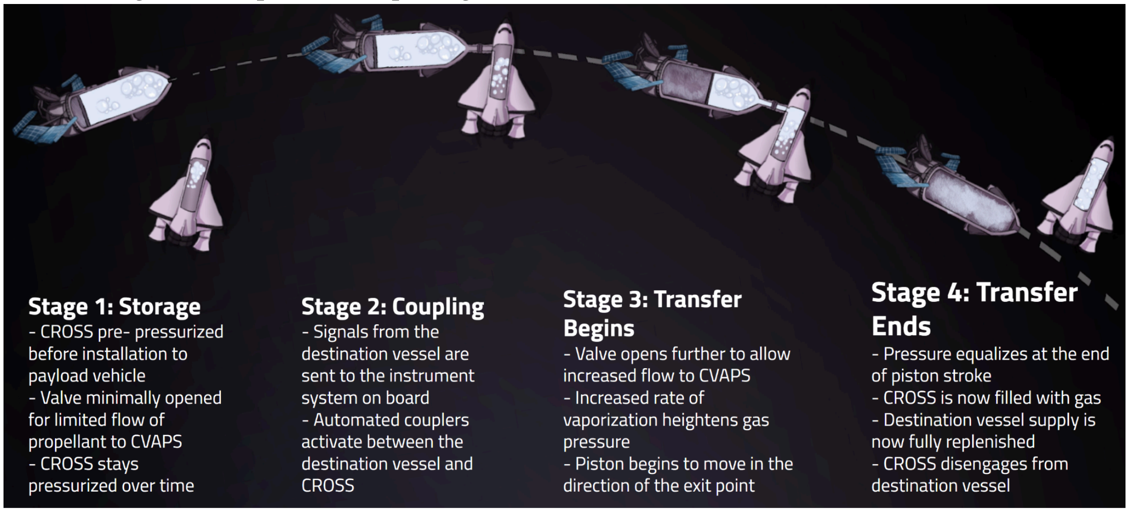

FIGURE 8: CROSS Concept of Operations

Conclusions

CROSS presents a novel yet practical solution for cryogenic propellant storage and transfer during extended space missions, including those under NASA's Artemis program. By integrating controlled autogenous pressurization into a classical piston-based positive expulsion device, Cross addresses key challenges associated with distributed launch missions. Its ability to provide a dynamically stabilized storage volume significantly reduces sloshing and slosh-inducing maneuvers—critical concerns in microgravity environments.

The system's simplified architecture, leveraging proven technologies and materials, supports long-duration propellant storage with minimal risk of contamination. The integration of thermoelectric modules enables advanced thermal regulation within the storage tank while providing propellant preheating conditions for CVAPS. While the design entails a slight reduction in expulsion efficiency, CROSS prioritizes system reliability, propellant purity, and maintainability over marginal performance gains.

In distributed launch scenarios—where several months may separate the launch of a storage module and the main vehicle—mission success depends on rapid turnaround and system readiness. Unlike the fuel tanks used in historical NASA missions, CROSS is designed for reusability.Its robust and straightforward design allows for multiple mission cycles with minimal maintenance or refurbishment, aligning with Artemis program goals and contributing to overall mission cost reduction.

Further development efforts should focus on optimizing the piston design to enhance thermal and structural robustness while reducing mass. Although currently, CROSS relies on established technologies, risks related to component failures—such as burst capillary lines, sensor malfunctions, or pump and compressor failures—remain. These concerns are mitigated through existing spaceflight redundancy strategies and maintenance protocols.

In conclusion, CROSS consolidates proven technologies into a cohesive and serviceable system with an estimated Technology Readiness Level (TRL) between 5 and 6. Continued development should prioritize mass optimization, cost-efficiency, and refinement of control systems—paving the way for reliable and sustainable in-space cryogenic fluid management.

Appendix

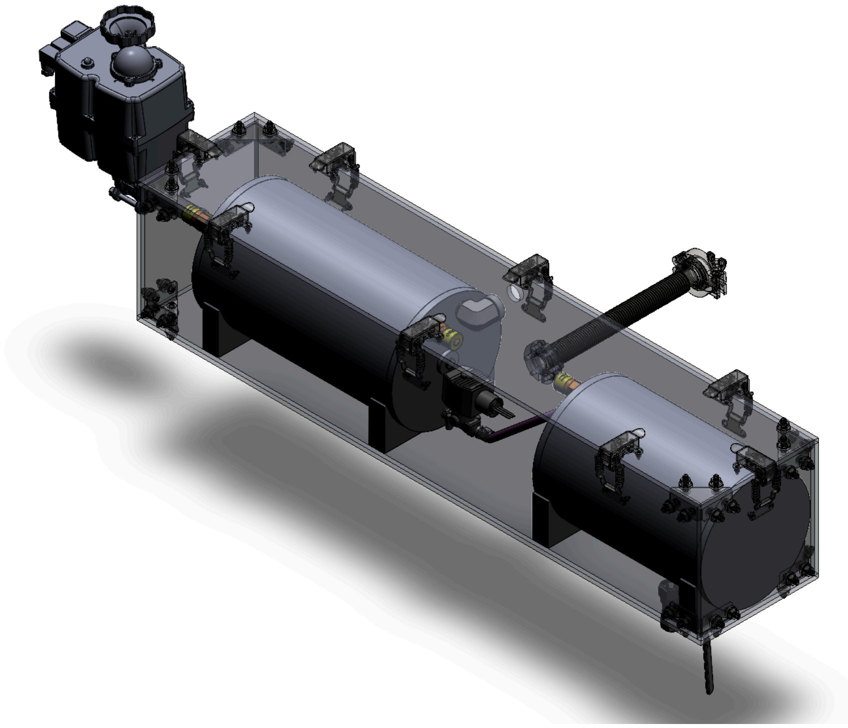

FIGURE A1: PULSE 3D Model Isometric View

FIGURE A2: PULSE SUB-A/B Setup

FIGURE A3: PULSE LND-T Setup

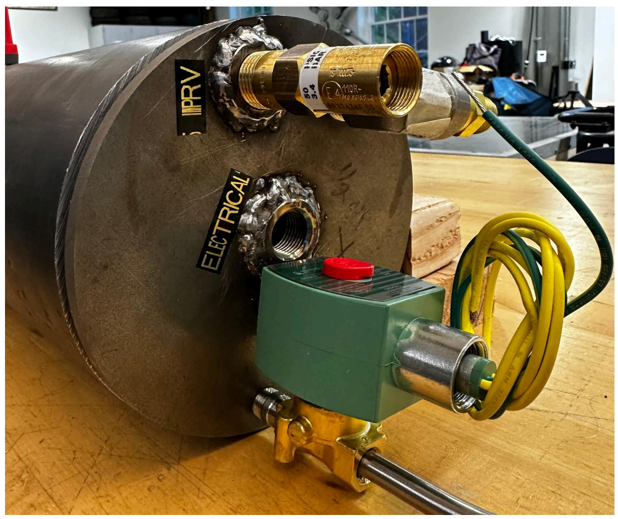

FIGURE A4: PULSE SUB-A/B with its Valves

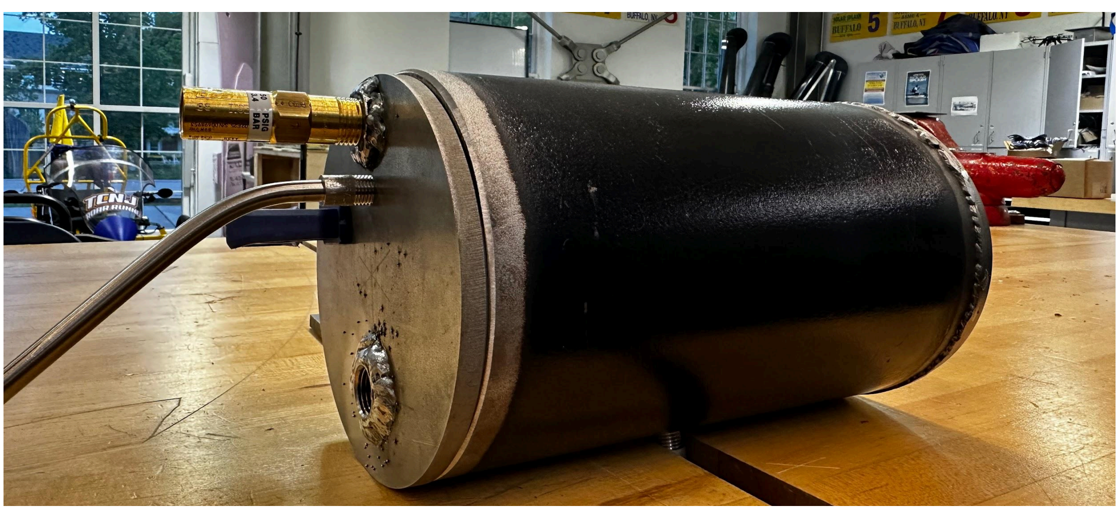

FIGURE A5: PULSE LND-T with its Valves

FIGURE A6: PULSE Mobility Unit

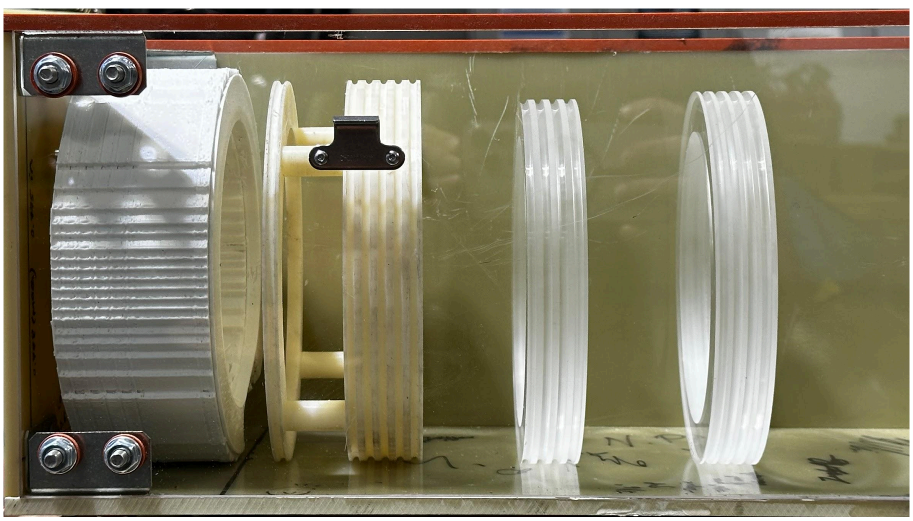

FIGURE A7: Piston Prototype Iterations

TABLE A1: Piston Ring Considerations

Ring Type	Material
Wear Ring Stock	Bronze Core and PTFE
PTFE Plastic	Solid PTFE Plastic
FEP	Rubber Core and FEP Plastic

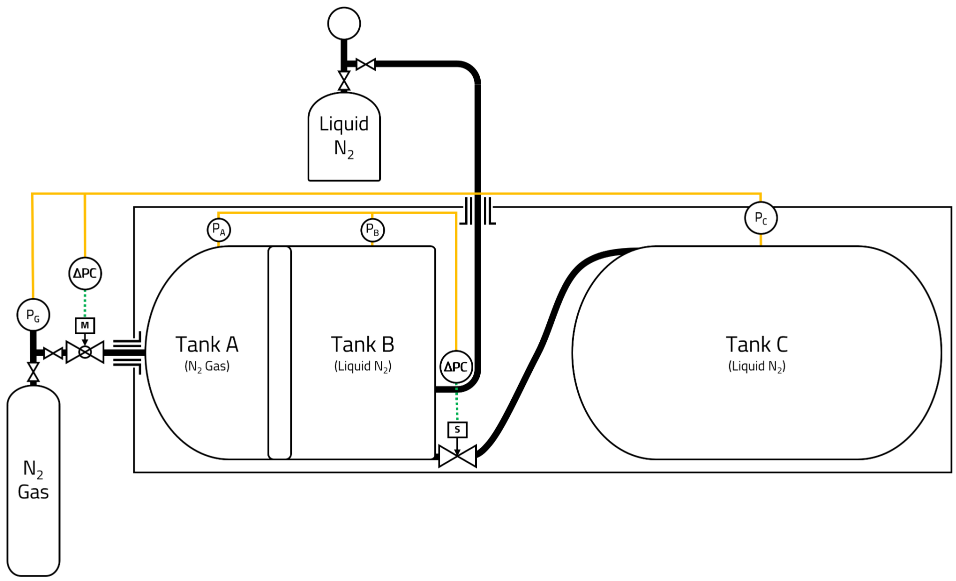

FIGURE A8: Mechanical P&ID for SCRIPT

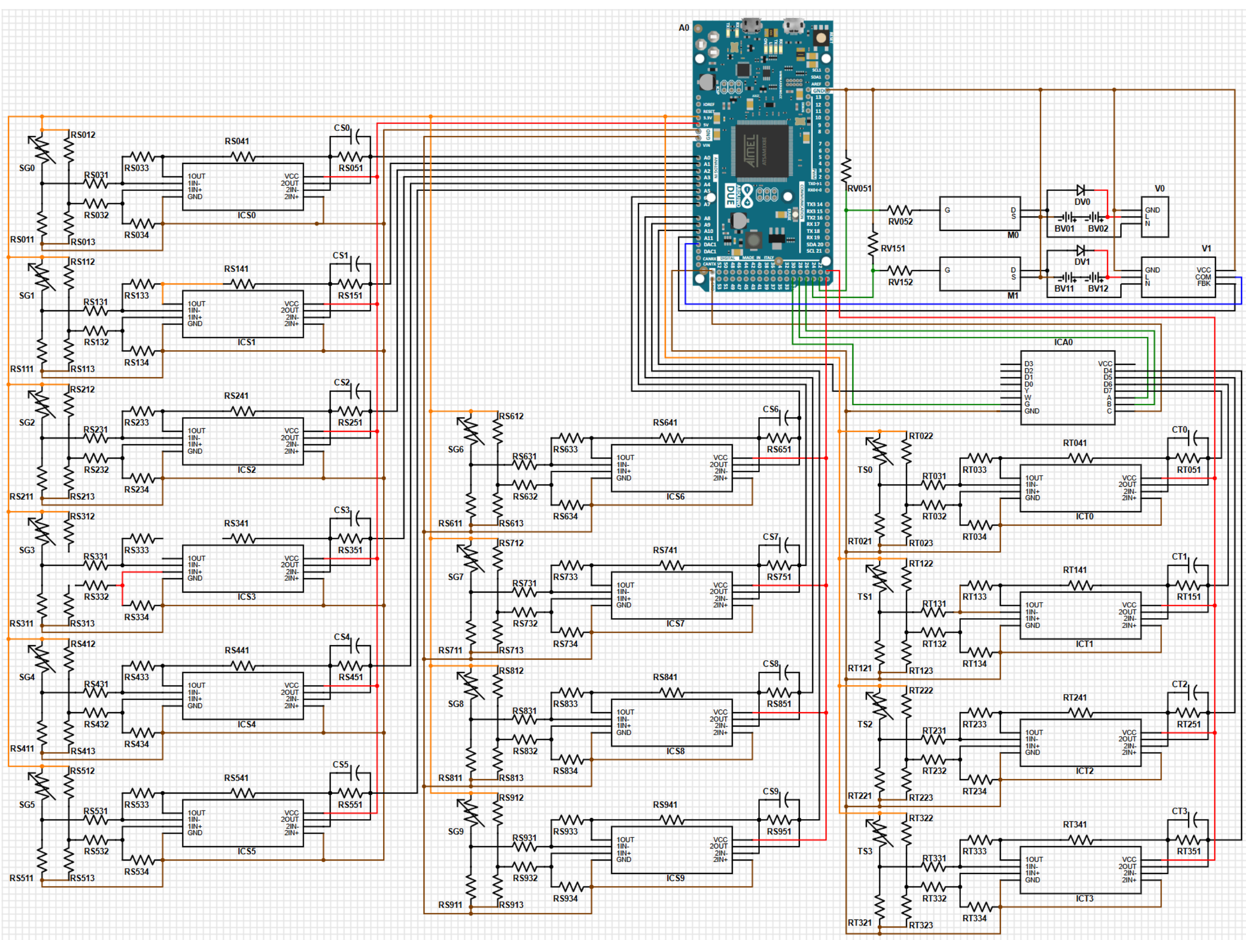

FIGURE A9: SCRIPT Wiring Diagram

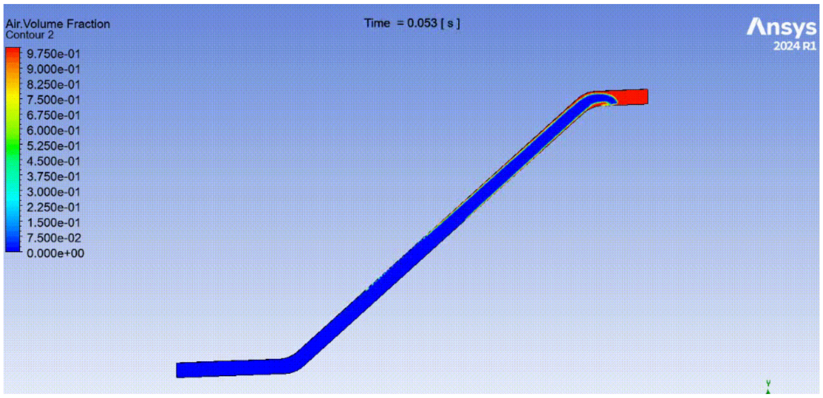

FIGURE A10: Transfer Line Flow Behavior

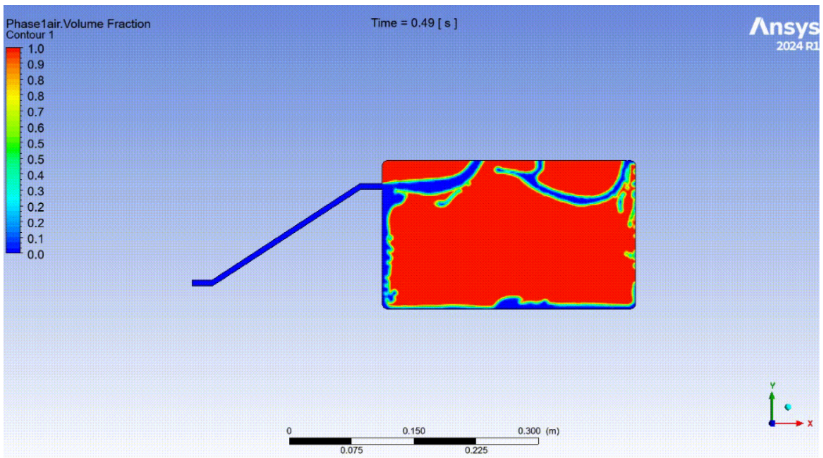

FIGURE A11: 5 m/s LND-T Flow

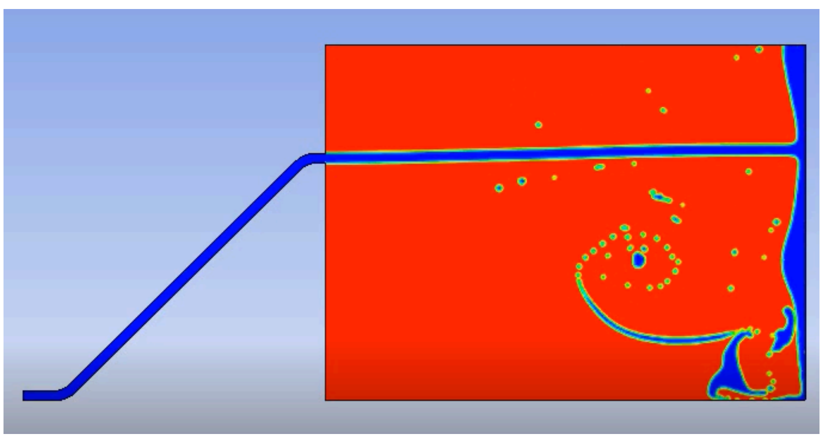

FIGURE A12: 15 m/s LND-T Flow

Task Name	Duration
Phase B	**280**
CROSS Preliminary Testing	**111**
CVAPS Prototype Construction	35
PULSE-2 Construction	30
Component Construction Margin	10
Prototype Integration	15
Component Integration Margin	5
In-Facility Prototype Testing	35
In-Facility Testing Margin	10
CROSS Microgravity Testing	**130**
Prototype ISS Transport Window	105
Microgravity Prototype Testing	55
Microgravity Testing Margin	20
CROSS PDR Development	**30**
PDR Development Margin	10
Phase C/D	**456**
CROSS Final Design Development	**71**
CVAPS Final Design Development	35
Storage Tank Final Design Development	25
Component Integration Design	20
Design Margin	15
CROSS CDR Development	**30**
CDR Development Margin	10
CVAPS Operations	**196**
CVAPS Parts Acquisition	35
CVAPS Build	50
CVAPS Assembly	30
CVAPS Testing	65
CVAPS Margin	15
Storage Tank Operations	**156**
Storage Tank Parts Acquisition	20
Storage Tank Build	35
Storage Tank Assembly	25
Storage Tank Testing	60
Storage Tank Margin	15
System Integration and Test Operations	**146**
SIT Integration	55
Integration Margin	15
SIT Testing	55
Testing Margin	15
CROSS Ready for Launch Delivery	**06/01/28**

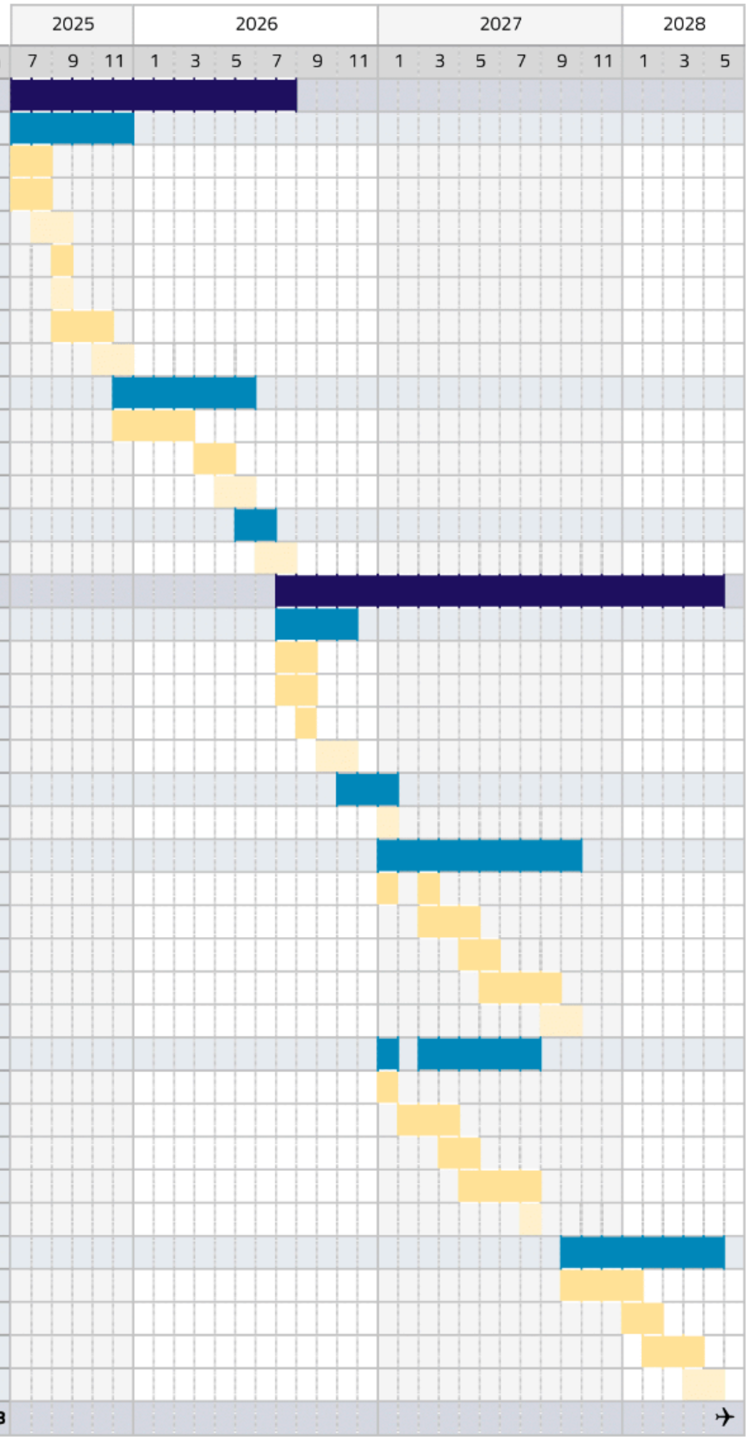

FIGURE A13: Proposed Path to Flight Timeline

References

Balasubramaniam, R., Ramé, E., & Motil, B. J. (2019). *Microgravity liquid-gas two-phase flow: Review of pressure drop and heat transfer correlations and guidelines for equipment operability* (NASA/TM–2019-220147). National Aeronautics and Space Administration. https://ntrs.nasa.gov/api/citations/20190001795/downloads/20190001795.pdf

Custom Heaters & Research. (n.d.). Custom Kapton polyimide flexible film heaters. https://customheatersandresearch.com/kapton-polyimide-heaters/

ERASMUS Centre - Directorate of Human Spaceflight and Operations. (n.d.). *Environment Control and Life Support System (ECLSS)* [Fact Sheet]. European Space Agency. https://wsn.spaceflight.esa.int/docs/Factsheets/30%20ECLSS%20LR.pdf

Gans, P. J. (1992, September). *Joule-Thomson Expansion*. [Lecture Notes]. https://tccc.iesl.forth.gr/education/local/Labs-PC-II/articles/JT.pdf

George C. Marshall Space Flight Center. (n.d.). *Cryogenic Fluid Management* [Fact Sheet]. National Aeronautics and Space Administration. https://www.nasa.gov/wp-content/uploads/2024/01/cryogenicfluidmanagement-factsheet.pdf?emrc=205323

George C. Marshall Space Flight Center. (2005). *External Tank Thermal Protection System* [Fact Sheet]. National Aeronautics and Space Administration. https://www.nasa.gov/wp-content/uploads/2016/08/114022main_tps_fs.pdf?emrc=b45d5a#:~:text=Though%20the%20foam%20insulation%20on,1.5%20to%203%20inches%20thick

Goodfellow. (2003, May 22). *Carbon/epoxy composite materials – properties – supplier data by Goodfellow*. AZoM. https://www.azom.com/article.aspx?ArticleID=1995

Hartwig, J. W. (2016). A Detailed Historical Review of Propellant Management Devices for Low Gravity Propellant Acquisition. *American Institute of Aeronautics and Astronautics*. https://doi.org/10.2514/6.2016-4772

Jenson, R. M., Weislogel, M. M., Tavan, N. T., Chen, Y., Semerjian, B., Bunnel, C. T., Collicott, S. H., Klatte, J., & Dreyer, M. E. (2009). The Capillary Flow Experiments Aboard the International Space Station: Increments 9–15 August 2004 to December 2007. https://ntrs.nasa.gov/api/citations/20090040689/downloads/20090040689.pdf

Kutter, B. F., Zegler, F., Sakla, S., Wall, J., Hopkins, J., Saks, G., Duffey, J., & Chato, D. J. (2006, November). *Settled cryogenic propellant transfer* (NASA Technical Memorandum No. NASA/TM-2006-214411; AIAA Paper 2006-4436). NASA Glenn Research Center. https://ntrs.nasa.gov/api/citations/20070001135/downloads/20070001135.pdf

Merino, J., Patzelt, A., Steinacher, A., Windisch, M., Heinrich, G., Forster, R., & Bauer, C. (2017). *Ariane 6 – Tanks and structures for the new European launcher*. Deutscher Luft- und Raumfahrtkongress 2017. https://www.dglr.de/publikationen/2017/450255.pdf

Mrozinski, J. (2020). NASA Instrument Cost Model (NICM) Version 9c. California Institute of Technology.

National Institute of Standards and Technology. (n.d.). NIST Chemistry WebBook. U.S. Department of Commerce. https://webbook.nist.gov/chemistry/

NASA Science Editorial Team. (2024). *Zero-Boil-Off Tank Experiments to Enable Long-Duration Space Exploration*. https://science.nasa.gov/science-research/science-enabling-technology/zero-boil-off-tank-experiments-to-enable-long-duration-space-exploration/

National Aeronautics and Space Administration. (2005). *External tank thermal protection system* (NASA Fact Sheet). NASA Marshall Space Flight Center. https://www.nasa.gov/wp-content/uploads/2016/08/114022main_tps_fs.pdf

Nast, T. C., Helvensteijn, B. P. M., Roth, E., Olson, J. R., Champagne, P., & Maddocks, J. R. (2014). *Cryocooler with cold compressor for deep space applications*. In S. D. Miller & R. G. Ross Jr. (Eds.), *Cryocoolers 18* (pp. 39–46). International Cryocooler Conference, Inc. https://www.cryocooler.org/resources/Documents/C18/006.pdf

Piñero, L. R., Peterson, P. Y., & Bowers, G. E. (2002). High Performance Power Module for Hall Effect Thrusters. https://ntrs.nasa.gov/api/citations/20030003703/downloads/20030003703.pdf

Rowe, D. M. (Ed.). (2006). *Thermoelectrics Handbook: Macro to Micro*. CRC Press.

Rudman, T. J., & Austad, K. L. (2002, December 3-6). *The Centaur Upper Stage Vehicle*. 4th International Conference on Launcher Technology “Space Launcher Liquid Propulsion”, Liege, Belgium. https://www.ulalaunch.com/docs/default-source/upper-stages/the-centaur-upper-stage-vehicle.pdf